

RSC Advances

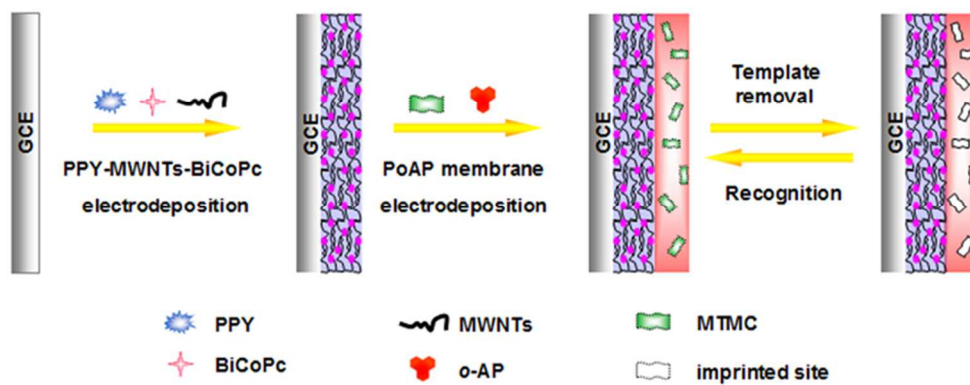


This is an *Accepted Manuscript*, which has been through the Royal Society of Chemistry peer review process and has been accepted for publication.

Accepted Manuscripts are published online shortly after acceptance, before technical editing, formatting and proof reading. Using this free service, authors can make their results available to the community, in citable form, before we publish the edited article. This *Accepted Manuscript* will be replaced by the edited, formatted and paginated article as soon as this is available.

You can find more information about *Accepted Manuscripts* in the [Information for Authors](#).

Please note that technical editing may introduce minor changes to the text and/or graphics, which may alter content. The journal's standard [Terms & Conditions](#) and the [Ethical guidelines](#) still apply. In no event shall the Royal Society of Chemistry be held responsible for any errors or omissions in this *Accepted Manuscript* or any consequences arising from the use of any information it contains.



Graphical Abstract

33x13mm (600 x 600 DPI)

13 **Abstract**

14 A molecularly imprinted electrochemical sensor for metolcarb (MTMC)
15 detection was designed and constructed by electropolymerizing a poly-*o*-aminophenol
16 (PoAP) membrane in the presence of MTMC after the modification of a composite
17 that consisted of polypyrrole (PPY), functionalized multiwalled carbon nanotubes
18 (MWNTs) and binuclear phthalocyanine cobalt (II) sulfonate (BiCoPc) on a glassy
19 carbon electrode (GCE) surface. The modified electrodes were characterized by
20 scanning electron microscopy (SEM) and cyclic voltammetry (CV). The molecularly
21 imprinted based sensor had a good binding ability toward MTMC upon measuring the
22 variation of the amperometric response of the oxidation-reduction probe, $K_3Fe(CN)_6$.
23 The relative peak current response was found to be proportional to the concentration
24 of MTMC in the range of 1.0×10^{-8} to 0.6×10^{-6} mol L⁻¹ with a detection limit of 7.88
25 $\times 10^{-9}$ mol L⁻¹ (S/N = 3). This desirable sensitivity may be attributed to the presence
26 of the PPY-MWNTs-BiCoPc composite layer, which enhanced the electrode surface
27 area and amplified the current signal. The sensor showed good selective affinity
28 toward MTMC, compared with similar molecules, with good reproducibility and
29 long-term stability. The prepared sensor was successfully applied to the determination
30 of MTMC residue in spiked vegetable samples with satisfactory recoveries ranging
31 from 88.8% to 93.3%.

32 **Keywords:** molecularly imprinted PoAP membrane, metolcarb, polypyrrole,
33 functionalized multiwalled carbon nanotubes, binuclear phthalocyanine cobalt (II)
34 sulfonate.

35 **1. Introduction**

36 The development of biological and chemical sensors for specific molecule
37 analysis has received considerable recent attention with research being conducted in
38 various fields including food safety [1], bioprocess control [2, 3], environmental
39 monitoring [4] and clinical field [5-7]. Their high selectivity toward target molecules
40 depends on the recognition element, which is usually derived from living organisms
41 like enzymes [8, 9] and antibodies [10, 11]. However, most of these materials are
42 expensive natural biomacromolecules and they generally have poor stability against
43 high temperatures, harsh chemical environments, or extreme pH conditions, and this
44 makes their wide application difficult.

45 Molecularly imprinted polymers (MIPs), also referred to as biomimetic
46 receptors, are artificial polymeric materials that have the ability to specifically bind
47 molecules with significant advantages in terms of ease of use and low preparation cost
48 as well as good mechanical and chemical stability under extreme conditions [12-14].
49 Therefore, MIPs may be used to overcome the limitations of biomacromolecules and
50 can be used as sensitive components in the development of biological and chemical
51 sensors [15-17]. For the construction of MIP-based sensors, in situ
52 electropolymerization is a promising method by which an ultrathin polymeric
53 membrane can be easily synthesized and adhered to a transducer surface of any shape,
54 size and thickness by controlling the amount of charge transferred [18-22]. However,
55 because of the high density and poor conductivity of electropolymerized molecularly
56 imprinted membranes, it will have fewer imprinted sites and a slow electron transfer

57 rate on modified electrode surfaces, which restricts the analytical efficiency of the
58 proposed MIP-based sensors.

59 Multiwalled carbon nanotubes (MWNTs), since their discovery in 1991, have
60 been the subject of comprehensive studies in various fields [23]. Owing to their
61 unique three-dimensional structures, high mechanical and chemical stability, large
62 surface-to-volume ratios, low resistivities and good biocompatibility, MWNTs can be
63 used as promising nanomaterials in the construction of electrochemical biosensors
64 because they increase the electrode's surface area and they facilitate electron transfer
65 [24-26]. Polypyrrole (PPY) is one of the most extensively studied conducting
66 polymers and has been widely used in the development of sensor devices because it
67 can be polymerized in a facile manner at neutral pH to form a stable membrane under
68 ambient conditions [27, 28]. To improve the efficiency and broaden the applications
69 of PPY, a dopant is usually part of the PPY polymer matrix [29]. Among the various
70 dopants, phthalocyanines, particularly binuclear phthalocyanines (such as binuclear
71 phthalocyanine cobalt (II) sulfonate, BiCoPc) are desirable because of their
72 large π electron conjugated system, excellent electron storage and transfer ability, and
73 their strong electrocatalytic behavior [30]. Producing a composite of PPY, MWNTs
74 and binuclear phthalocyanine should combine the advantages of these materials.
75 Composite materials may possess complementary properties because of synergistic
76 effects and thus increase the total performance of the sensing component.

77 Metolcarb (MTMC) is an important N-methylcarbamate pesticide and is widely
78 used in agricultural production because of its broad spectrum of activity and low

79 bioaccumulation potential [31]. However, its pesticidal action results from the
80 inhibition of acetylcholinesterase transmission at nerve endings is potentially
81 hazardous to human health [32, 33]. Until recently, analytical methods for MTMC
82 residue determination in agricultural products were generally based on
83 chromatography [34, 35] and immunoassays [36, 37]. Although these methods are
84 sensitive and specific, a number of shortcomings still restrict their practical use and
85 these include expensive instrumentation, time-consuming procedures, and the poor
86 chemical or physical stability of antibodies and enzymes. The development of an
87 inexpensive, rapid and stable but sensitive method for MTMC residue analysis is still
88 a challenge.

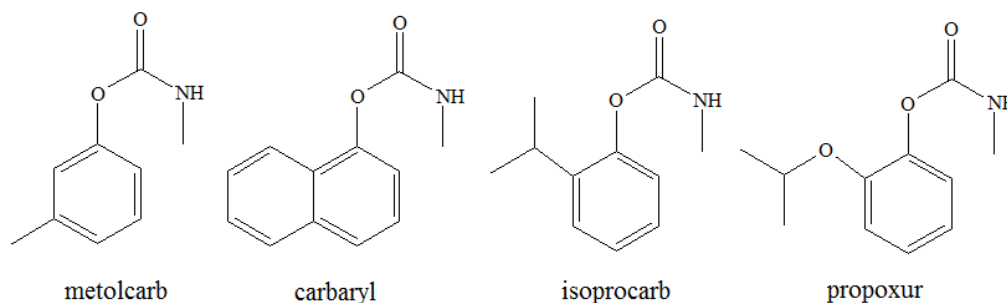
89 We thus report a rapid electrochemical strategy for MTMC determination by
90 electrodepositing a molecularly imprinted poly-*o*-aminophenol (PoAP) membrane on
91 a GC electrode surface modified with a PPY-MWNTs-BiCoPc composite. As far as we
92 know, this is the first attempt to fix the PPY-MWNTs-BiCoPc composite material onto
93 the surface of a GC electrode to construct a MIP-based sensor. The resultant sensor
94 demonstrated that the modified composite layer can effectively improve the
95 performance of the imprinted electrodeposited membrane to provide a more sensitive
96 analysis of MTMC.

97 **2.1 Reagents and chemicals**

98 Pyrrole, template MTMC, and the other analytes tested including carbaryl,
99 isoprocarb and propoxur (Fig. 1) were purchased from Sigma–Aldrich (Madrid,
100 Spain). *o*AP, MWNTs and BiCoPc were purchased from Alfa Aesar (Tianjin, China),

101 Shenzhen Nanotech Port Co., Ltd. (Shenzhen, China) and Shanghai Dibo Chemical
102 Technology Co., Ltd., (Shanghai, China), respectively. Potassium ferricyanide
103 ($K_3[Fe(CN)_6]$) and the other chemicals used in our experiments were purchased from
104 Tianjin No. 1 Chemical Reagent Factory (Tianjin, China) and were of analytical grade.
105 Doubly deionized water (DDW, $18.2\text{ M}\Omega\text{ cm}$) was used throughout and was obtained
106 from a Water Pro water purification system (Labconco, Kansas City, USA).

107 Stock solutions of the individual analytes (MTMC, carbaryl, isoprocarb and
108 propoxur) were prepared in methanol with a concentration of 1.0 mmol L^{-1} and stored
109 at $4\text{ }^\circ\text{C}$. The corresponding working solutions were obtained by diluting the individual
110 stock solutions with DDW.



111

112 *Fig.1 Chemical structures of MTMC, carbaryl, isoprocarb and propoxur*113 **2.2 Apparatus**

114 All the electrochemical experiments were carried out at room temperature using a
115 LK 2006 electrochemical workstation (Tianjin Lanlike Chemical and Electronic High
116 Technology Co., Ltd., China) connected to a personal computer. A typical
117 three-electrode configuration was employed consisting of a bare or modified GC
118 electrode as the working electrode, a saturated calomel electrode (SCE) and platinum
119 foil as the reference electrode and counter electrode, respectively. Scanning electron

120 microscopy (SEM, SU1510, Hitachi, Japan) was used to observe the morphology of
121 the surface of various modified electrodes.

122 **2.3 Preparation of the Imprinted PoAP-PPY-MWNTs-BiCoPc-GC**

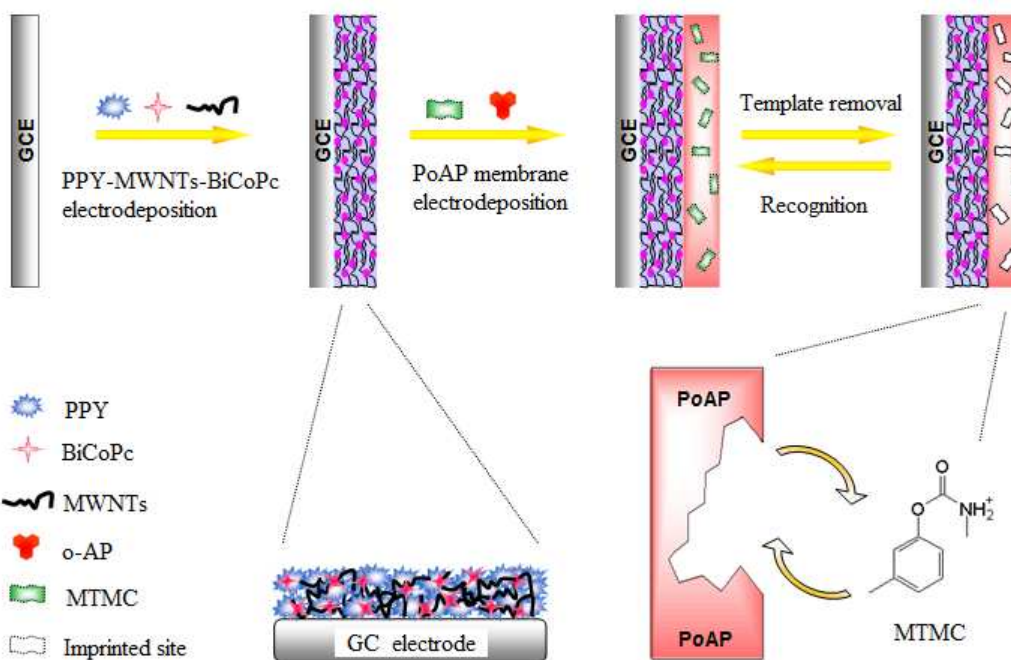
123 **Electrode**

124 500.0 mg of crude MWNTs were added to 60.0 mL of concentrated HNO₃ under
125 sonication for 10 min. The mixture was then refluxed under stirring at 85 °C for 12 h.
126 After cooling to room temperature, the mixture was separated by filtering through a
127 0.22 µm polycarbonate membrane and it was washed thoroughly with DDW until the
128 pH was neutral. The obtained solid product was denoted MWNTs-COOH, and it was
129 found to enhance the dispersion and stability of the crude MWNTs [34].

130 The preparation of the PPY-MWNTs-BiCoPc-GC electrode was conducted as
131 follows: the bare GC electrode (d = 4 mm) was polished carefully to a mirror-like
132 surface with 0.3-0.05 µm alumina aqueous slurry and it was then successively cleaned
133 with nitric acid (1:1, v/v), ethanol and DDW. MWNTs-COOH (6.0 mg) was dispersed
134 into the pyrrole aqueous solution (50.0 mmol L⁻¹, 6.0 mL) containing BiCoPc (6.0
135 mg). After sonication for 1 h, chronoamperometry was employed to electrodeposit the
136 PPY-MWNTs-BiCoPc composite onto the bare GC electrode surface by immersing
137 the electrode in the above-mentioned solution using a constant potential of 0.7 V for
138 180 s. Additionally, we prepared a PPY-GC electrode, a PPY-MWNTs-GC electrode
139 and a PPY-BiCoPc-GC electrode using the same conditions as above in a relevant
140 solution.

141 To electrochemically synthesize a PoAP membrane onto the surface of the

142 PPY-MWNTs-BiCoPc composite the resulting electrode was immersed in a
 143 N₂-deoxygenated perchloric acid solution (0.1 mol L⁻¹, pH 5.5) containing *o*AP (20.0
 144 mmol L⁻¹), MTMC (10.0 mmol L⁻¹) with a small amount of methanol as cosolvent
 145 because of the poor solubility of MTMC in water. The electropolymerization was
 146 performed by eight consecutive cyclic voltammetry scans over the potential range of
 147 -0.1 - 0.8 V (versus the SCE) at a scan rate of 50 mV s⁻¹. After the
 148 electropolymerization, the PoAP membrane modified PPY-MWNTs-BiCoPc-GC
 149 electrode was rinsed with a water:methanol solution (4:6, v/v) three times for 30 min
 150 each to remove the template molecules trapped within the polymer matrix. Control
 151 studies were performed by fabricating a non-imprinted
 152 PoAP-PPY-MWNTs-BiCoPc-GC electrode without an additional template during
 153 electropolymerization. A schematic diagram of the whole imprinted sensor
 154 preparation procedure is shown in Fig. 2.



155

156 *Fig. 2 Preparation procedure for the imprinted PPY-MWNTs-BiCoPc-GC electrode*

157 **2.4 Measurement experiments**

158 Cyclic voltammetry (CV) was used to characterize the different modified
159 electrodes and to evaluate the rebinding of MTMC onto the imprinted and
160 non-imprinted PPY-MWNTs-BiCoPc-GC electrodes. The CV experiments were
161 performed from -0.2 to +0.6 V at a scan rate of 100 mV s⁻¹ in a standard solution of
162 K₃[Fe(CN)₆] (1.0 mmol L⁻¹) containing KNO₃ (0.2 mol L⁻¹). In the template rebinding
163 experiments, when the initial current response was stable, a small aliquot of analyte
164 solution was injected by microsyringe and the resulting current responses were
165 recorded and used for data analysis. All measurements were taken at room
166 temperature.

167 **2.5. Sample preparation**

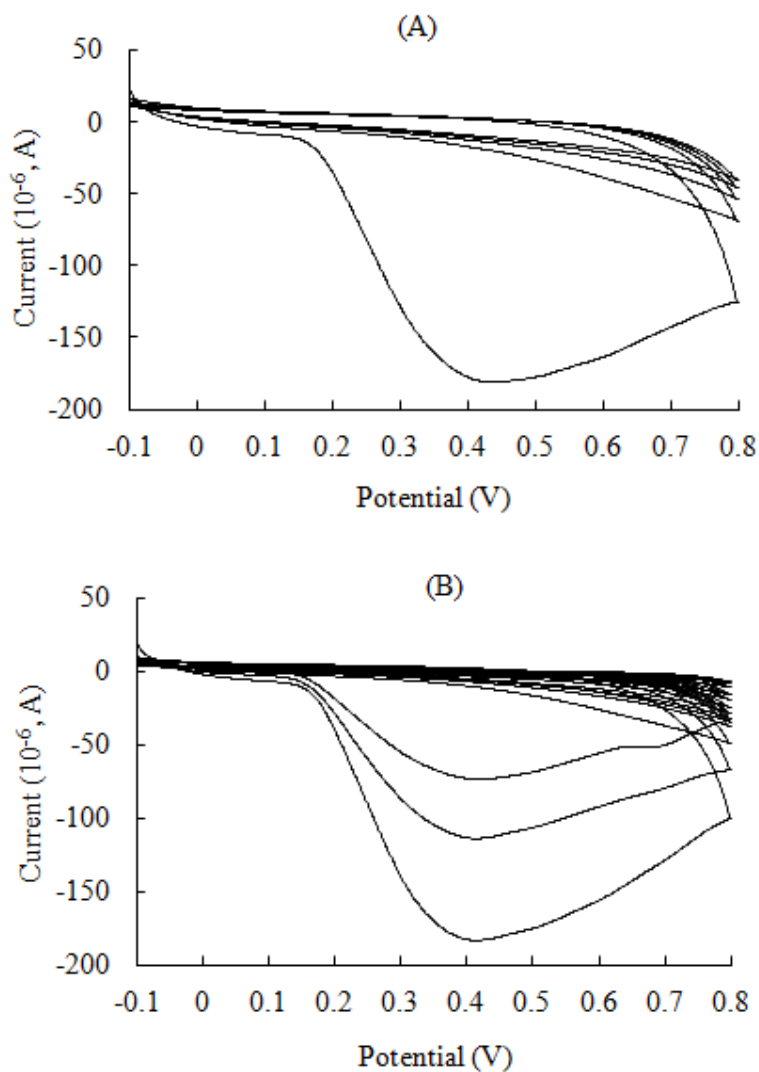
168 Cucumber and cabbage samples obtained from a local market were determined to
169 be free of MTMC by HPLC and were used to perform spiking and recovery studies.
170 The samples were cut and then 2.0 g of a sample was packed into a 50 mL
171 polypropylene centrifuge tube and spiked with MTMC at 40.0 µg kg⁻¹, 200.0 µg kg⁻¹,
172 and 400.0 µg kg⁻¹. 10.0 mL methanol was added to the tube and it was thoroughly
173 shaken (5 min). The obtained mixture was centrifuged at 4000 rpm for 10 min. The
174 extraction procedure was repeated twice and the supernatant was combined and
175 evaporated to dryness at 60 °C under reduced pressure. Finally, the dried extract was
176 redissolved in 10.0 mL of 5% methanol-standard K₃[Fe(CN)₆] solution and filtered
177 using a 0.22 µm filter before electrochemical analysis.

178 **3. Results and discussion**

179 **3.1. Molecular imprinting electropolymerization**

180 Figure 3A shows representative cyclic voltammograms during the *PoAP*
181 membrane electropolymerization process at the PPY-MWNTs-BiCoPc-GC electrode
182 surface in the presence of MTMC. A large *oAP* anodic peak was observed at a
183 potential of 0.43 V in the first positive-direction potential scan and it completely
184 disappeared in the second anodic scan. No cathodic peak was obtained during the
185 negative-direction potential scan. These results suggest that the process was an
186 entirely irreversible oxidation process and that the active groups ($-\text{NH}^{3+}$) of *oAP* can
187 be utilized to immobilize the template molecules during the positive potential scan
188 [39]. The current intensity decreased sharply under continuous cyclic scanning and
189 stabilized after five cycles and this seems to be related to the progressive formation of
190 an insulating *PoAP* membrane that covers the surface of the
191 PPY-MWNTs-BiCoPc-GC electrode leading to a suppression of the voltammetric
192 response. No significant differences were observed for the cyclic voltammograms in
193 the presence or absence (Fig. 3B, curve c) of MTMC, which indicates that MTMC did
194 not show electrochemical activity in the chosen potential window. Therefore, its
195 structure was not electrochemically altered during electropolymerization. Additionally,
196 the cyclic voltammograms for the electropolymerization of the *PoAP* membrane on
197 the PPY-MWNTs-BiCoPc-GC electrode exhibited the highest anodic peak current (\approx
198 180 μA) compared with the membrane electrodeposited onto the bare GC electrode
199 (Fig. 3B, curve a, \approx 70 μA) and the PPY-BiCoPc-GC electrode (Fig. 3B, curve b, \approx

200 120 μA). This high anodic peak current can be explained by the excellent electrical
201 conductivity and large surface area of the modified PPY-MWNTs-BiCoPc composite
202 layer.



203

204

205 *Fig. 3 (A) Cyclic voltammograms for the electropolymerization of the PoAP membrane at the*
206 *surface of the PPY-MWNTs-BiCoPc-GC electrode in the presence of MTMC. Scan rate: 50 mV s^{-1} ,*
207 *cycle number: 5. (B) Cyclic voltammograms for the electropolymerization of the PoAP membrane*
208 *at the surface of (a) the bare GC electrode, (b) the PPY-BiCoPc-GC electrode, and (c) the*
209 *PPY-MWNTs-BiCoPc-GC electrode in the MTMC absence. Scan rate: 50 mV s^{-1} , cycle number: 8.*

210 **3.2. Characteristics of the modified electrode**

211 **3.2.1. Morphological characterization**

212 The surface morphology of the various modified electrodes were compared by
213 SEM. Fig. 4A shows a SEM image of the PPY-MWNTs-GC electrode and it is clear
214 that the MWNTs were distributed over the GC electrode surface with a typically
215 three-dimensional tubular structure and numerous clusters were formed, indicating
216 that the MWNTs tend to aggregate in the PPY layer. When BiCoPc was doped into
217 the PPY layer, a vastly different morphology results (Fig. 4B) as the homogeneous
218 PPY layer contains a larger amount and more uniform MWNTs. This rough composite
219 layer structure increased the electrode surface area and influenced the amount of
220 imprinted sites formed for the following electropolymerization. As shown in Fig. 4C,
221 after the electrodeposition of the PoAP membrane at the surface of the
222 PPY-MWNTs-GC electrode the size of the network structures composed of MWNTs
223 and BiCoPc increased remarkably. This can be explained by the sufficient
224 encapsulation of the composite layer by the polymer membrane. These results
225 demonstrated that the PoAP membrane was easily electrochemically deposited onto
226 the PPY-MWNTs-BiCoPc composite layer surface with the formation of many rough
227 network structures. The resulting modified electrode therefore had a large specific
228 surface area for binding to target molecules.

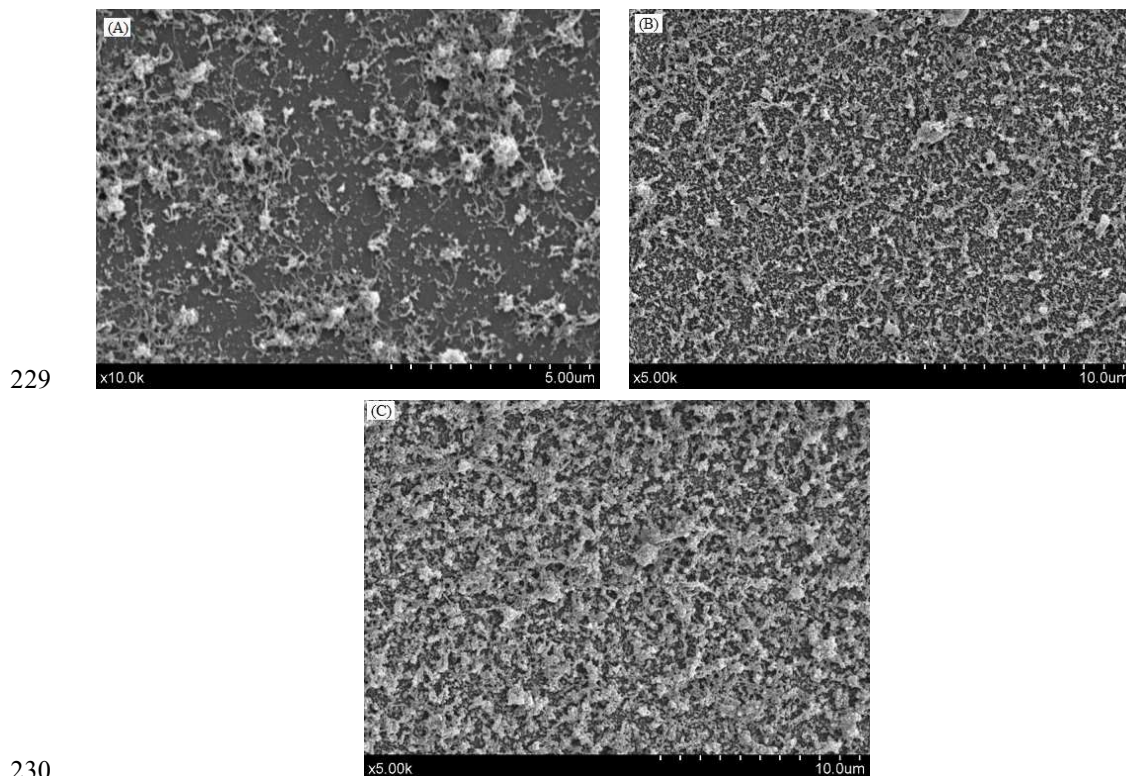
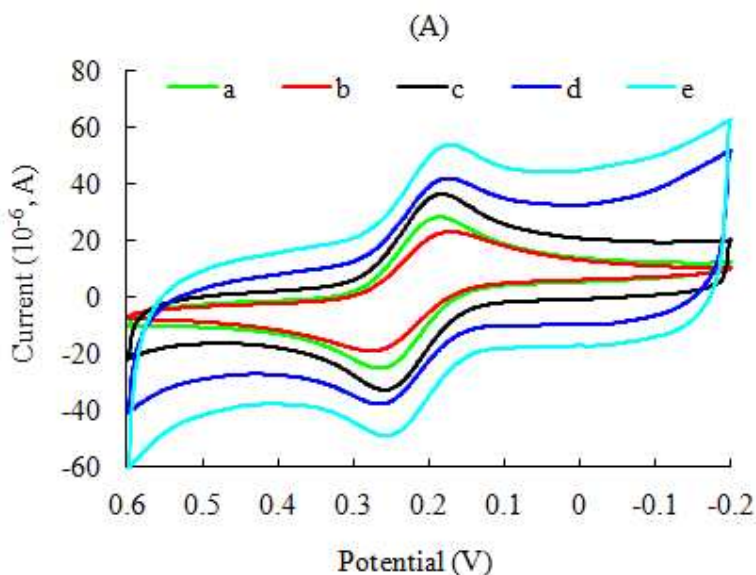


Fig. 4 SEM images of the surfaces of (A) the PPY-MWNTs-GC electrode, (B) the PPY-MWNTs-BiCoPc-GC electrode and (C) the PPY-MWNTs-BiCoPc-GC electrode after the electrodeposition of the PoAP membrane

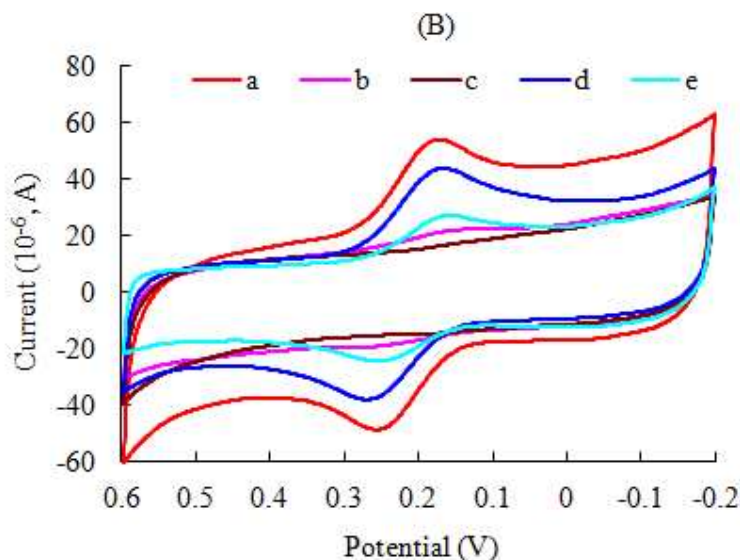
234 **3.2.2. Electrochemical characteristics of the PPY-MWNTs-BiCoPc** 235 **composite layer**

236 Cyclic voltammetry is a convenient and effective method to investigate electron
237 transfer in surface modified electrodes [40]. In this work, the electrochemical
238 behavior of the electrodes prepared using different modification processes was studied
239 in a 1.0 mmol L⁻¹ K₃[Fe(CN)₆] solution containing 0.2 mmol L⁻¹ KNO₃. A comparison
240 of the cyclic voltammograms of the bare GC electrode, the PPY-GC electrode, the
241 PPY-MWNTs-GC electrode, the PPY-BiCoPc-GC electrode and the
242 PPY-MWNTs-BiCoPc-GC electrode is shown in Fig. 5A. The cyclic voltammogram

243 of the bare GC electrode showed a typical quasi-reversible electrochemical reaction
244 with a couple of redox peaks (curve a). After PPY was polymerized onto the GC
245 electrode's surface (curve b) its reversibility deteriorated indicating that a compact
246 PPY layer was formed and this passivated the electrode surface. When the MWNTs
247 (curve c) and BiCoPc (curve d) were doped into PPY by electropolymerization the
248 redox peak currents of the obtained electrodes increased significantly. However, a
249 maximum peak current was observed only when the MWNTs and BiCoPc were doped
250 simultaneously (curve e). This result can be attributed to a synergistic effect in the
251 modified PPY-MWNTs-BiCoPc composite layer wherein the electron transfer rate
252 accelerated and the effective area of the electrode surface increased.



253



254
 255 Fig. 5 (A) Cyclic voltammograms of (a) the bare GC electrode, (b) the PPY-GC electrode, (c) the
 256 PPY-MWNTs-GC electrode, (d) the PPY-BiCoPc-GC electrode and (e) the
 257 PPY-MWNTs-BiCoPc-GC electrode in an aqueous solution consisting of $1.0 \text{ mmol L}^{-1} \text{ K}_3[\text{Fe}(\text{CN})_6]$
 258 and $0.2 \text{ mol L}^{-1} \text{ KNO}_3$. Scan rate: 100 mV s^{-1} . (B) Cyclic voltammograms of (a) the
 259 PPY-MWNTs-BiCoPc-GC electrode, (b) the non-imprinted PoAP-PPY-MWNTs-BiCoPc-GC
 260 electrode, the imprinted PoAP-PPY-MWNTs-BiCoPc-GC electrode (c) before and (d) after
 261 removing the template MTMC and (e) the imprinted PoAP-PPY-MWNTs-BiCoPc-GC electrode
 262 after incubating with $6 \times 10^{-7} \text{ mol L}^{-1} \text{ MTMC}$ and obtained from a $1.0 \text{ mmol L}^{-1} \text{ K}_3[\text{Fe}(\text{CN})_6]$
 263 solution containing $0.2 \text{ mmol L}^{-1} \text{ KNO}_3$. Scan rate: 100 mV s^{-1} .

264 3.2.3. Electrochemical characteristics of the imprinted and the 265 non-imprinted electrodes

266 The cyclic voltammograms of the PPY-MWNTs-BiCoPc-GC electrode and the
 267 various PoAP membrane modified PPY-MWNTs-BiCoPc-GC electrodes were
 268 compared and are shown in Fig. 5B. As shown in curve a, the
 269 PPY-MWNTs-BiCoPc-GC electrode showed a remarkable current response with a

270 couple of redox peaks. After modification with the non-imprinted P α AP membrane
271 only a small peak current was observed (curve b) because of the formation of a
272 non-conducting P α AP membrane that covered the surface of the
273 PPY-MWNTs-BiCoPc-GC electrode. This hindered the electron transfer pathways.
274 However, for the imprinted PPY-MWNTs-BiCoPc-GC electrode, the redox peaks
275 were restored after the template elution process (curve c and curve d), which suggests
276 that cavities were produced in the imprinted P α AP membrane after MTMC removal.
277 [Fe(CN) $_6$] $^{3-}$ could diffuse through these cavities toward the surface of the electrode
278 resulting in a redox reaction. Furthermore, after immersing the imprinted
279 PPY-MWNTs-BiCoPc-GC electrode in 6.0×10^{-7} mol L $^{-1}$ MTMC, the redox peak
280 currents decreased obviously (curve e), which can be explained by the rebinding of
281 MTMC onto the produced imprinted cavities, which blocks the arrival of [Fe(CN) $_6$] $^{3-}$
282 on the electrode surface.

283 **3.3. Optimization of the imprinted P α AP-PPY-MWNTs-BiCoPc-GC** 284 **electrode's preparation conditions**

285 The constitution of the PPY-MWNTs-BiCoPc composite layer will affect the
286 electrochemical performance of the modified electrode and, therefore, we optimized
287 the amount of MWNTs and BiCoPc doped into the PPY layer at different ratios
288 (BiCoPc/MWNTs ratio, 1:4, 1:2, 1:1, 3:2, 2:1 and the concentration of MWNTs was
289 fixed at 1 mg mL $^{-1}$). We found that the redox peak currents of Fe(CN) $_6^{3-/4-}$ increased
290 significant at BiCoPc/MWNTs ratios up to 1:1 after which they tended to be flat. The
291 growth interface conductivity may be attributed to a composite action between

292 BiCoPc and MWNTs through π - π interactions which reduces the aggregation of
293 MWNTs and improves the properties of the PPY lay. However, excessive BiCoPc
294 doping and excessive deposition time will generate a polarization phenomenon in the
295 PPY-BiCoPc leading to the poor stability of the current response. As a result, a
296 BiCoPc/MWNTs ratio of 1:1 and a deposition time of 180 s were selected to prepare
297 the composite layer for electrode modification.

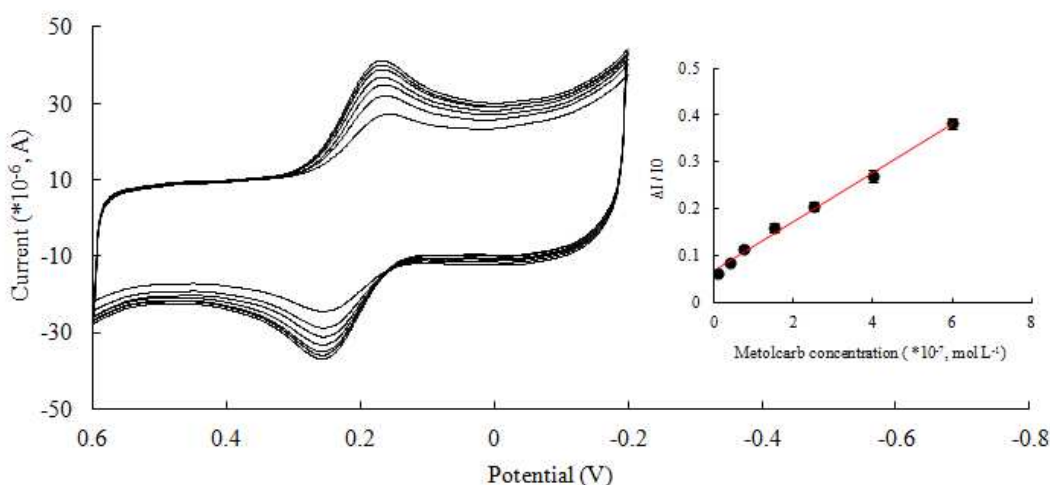
298 For the construction of a MTMC imprinted PoAP membrane, the amount of
299 imprinted sites available for the selective rebinding template molecules is directly
300 influenced by the ratio of template to monomer in the electropolymerization solution.
301 To determine the most suitable ratio, the PoAP membranes were synthesized and
302 compared using template:monomer molar ratios of 1:1, 1:2 and 1:3. The results show
303 that the membrane synthesized at a ratio of 1:2 exhibited the largest current response
304 change and the shortest adsorption equilibrium time during CV analysis. Therefore, it
305 was chosen for the following experiments.

306 The thickness of the imprinted polymer membrane was a critical parameter that
307 affected the permeation rate and stability of the recognition element. Although more
308 PoAP deposition can embed more of the template molecule and give better membrane
309 stability, the incomplete removal of the template from an excessively thick membrane
310 will reduce the number of accessible imprinted sites and finally result in low binding
311 capacity and slow binding kinetics [41, 42]. Because of the use of the
312 electrodeposition method, the thickness of the PoAP membrane is easily controlled by
313 adjusting the number of CV scanning cycles. We found that the current response

314 change for the imprinted PoAP-PPY-MWNTs-BiCoPc-GC electrode toward the same
315 concentration of MTMC increased with CV cycle number up to eight cycles and it
316 then decreased gradually with additional cycles. Thus, eight cycles were chosen for
317 the electrodeposition of the PoAP membrane to give a suitable thickness for MTMC
318 detection.

319 **3.4 Evaluation of the binding performance of the imprinted** 320 **PoAP-PPY-MWNTs-BiCoPc-GC electrode**

321 The binding affinity of the imprinted PoAP-PPY-MWNTs-BiCoPc-GC
322 electrode toward MTMC was evaluated by measuring the CV response upon the
323 addition of the MTMC working solution.



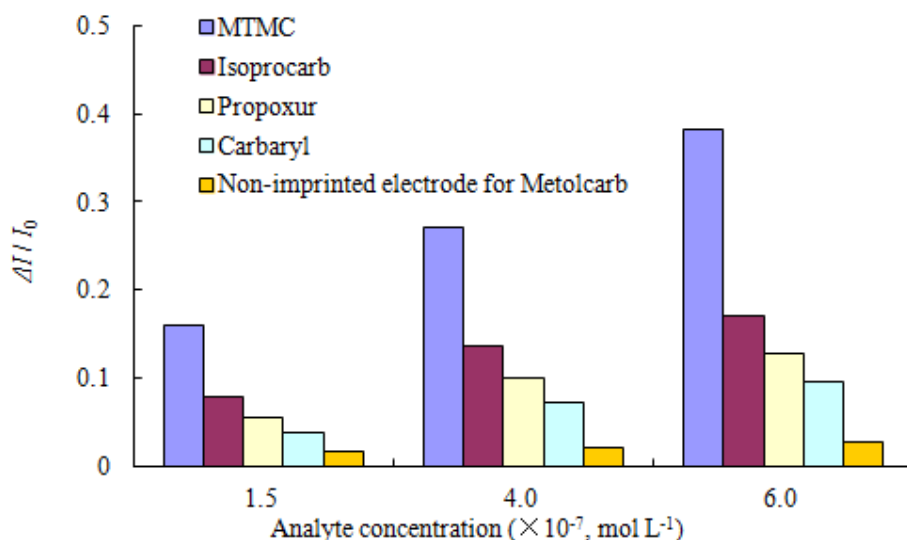
324
325 *Fig. 6 Cyclic voltammograms of the imprinted PoAP-PPY-MWNTs-BiCoPc-GC electrode in*
326 *response to different concentrations of MTMC. Scan rate: 100 mV s $^{-1}$. Inset: linear relationships of*
327 *the relative current change vs. MTMC concentrations.*

328 As shown in Fig. 6, an increase in the concentration of MTMC leads to a
329 significant decrease in current response, indicating that the increased adsorption of

330 MTMC molecules onto the imprinted electrode surface hinders the diffusion of the
331 probe $[\text{Fe}(\text{CN})_6]^{3-}$. When the concentration is high the change in current tends to
332 stabilize, and this can be attributed to the sufficient occupation of imprinted cavities
333 by MTMC molecules. The relative current change is defined as $\Delta I/I_0$, where $\Delta I = I_0 -$
334 I_c is the change in anodic peak current, and I_0 , I_c refer to the anodic peak current
335 values at analyte concentrations of 0 and $c \text{ mol L}^{-1}$, respectively. The results show that
336 the relative current change is proportional to the concentration of MTMC in the range
337 of 1.0×10^{-8} to $0.6 \times 10^{-6} \text{ mol L}^{-1}$ with a correlation coefficient of 0.9938 (Fig. 6,
338 inset). The limit of detection (LOD, S/N = 3) was calculated to be $7.88 \times 10^{-9} \text{ mol L}^{-1}$
339 (about $1.3 \mu\text{g L}^{-1}$), which could be comparable with the results of chromatographic
340 method with more than $6.455 \mu\text{g kg}^{-1}$ [35] and immunoassay with $1.2 \mu\text{g L}^{-1}$ [36] and
341 biomimetic sensing with $2.21 \mu\text{g L}^{-1}$ [43]. On the contrary, the decrease in the
342 response current was much lower and independent by comparison with the imprinted
343 electrode when the non-imprinted electrode was used as the working electrode (Fig. 7).
344 This may be because the non-imprinted electrode lacked suitable imprinted sites for
345 MTMC binding. Moreover, the imprinted *PoAP*-PPY-MWNTs-BiCoPc-GC electrode
346 also had a shorter equilibrium time ($\approx 8 \text{ min}$) for analyte measurements. The rapid
347 adsorption equilibrium characteristic is attributed to the electrodeposition of *PoAP*
348 onto a very rough PPY-MWNTs-BiCoPc composite layer, which enhances the
349 penetration of the analyte into the imprinted *PoAP* membrane (Fig. 4C).

350 **3.5. Selectivity experiment**

351 The selectivity of the proposed sensor, based on the specific binding
 352 interactions between the analyte and the recognition sites is an important
 353 characteristic that should be investigated. In this study, compounds with structures
 354 similar to MTMC such as isoprocarb, propoxur and carbaryl were used to evaluate the
 355 current response of the imprinted *PoAP-PPY-MWNTs-BiCoPc-GC* electrode at a
 356 series of analyte concentrations (1.5×10^{-7} , 4.0×10^{-7} , 6.0×10^{-7} mol L⁻¹). For
 357 simplicity, we define the selectivity coefficient (SC) as $SC = \alpha_{\text{MTMC}} / \alpha_{\text{analyte}}$, where α
 358 is the gradient of the respective linear curves for the different analytes.



359

360 *Fig. 7 Relative current change corresponding to the imprinted*361 *PoAP-PPY-MWNTs-BiCoPc-GC electrode for different concentrations of MTMC, carbaryl,*362 *isoprocarb and propoxur and the non-imprinted PoAP-PPY-MWNTs-BiCoPc-GC electrode for the*363 *determination of MTMC.*

364 As shown in Fig. 7, the analytes isoprocarb, propoxur and carbaryl exhibited
 365 less relative current changes than MTMC with SC values of 2.45, 3.06 and 3.95,
 366 respectively. This indicates good selectivity of the imprinted

367 *PoAP*-PPY-MWNTs-BiCoPc-GC electrode toward the template molecule over its
368 structural analogs. Moreover, the relatively high current changes for isoprocab
369 compared with the other two analogs in the selectivity experiment is attributed to its
370 structure being more similar to MTMC and its smaller steric hindrance, which enabled
371 it to easily enter the imprinted cavities in the *PoAP* membrane.

372 **3.6. Reproducibility and stability**

373 The reproducibility of the imprinted *PoAP*-PPY-MWNTs-BiCoPc-GC electrode
374 was estimated by detection the current response at a controlled MTMC concentration
375 of 1.5×10^{-7} mol L⁻¹. The measurements were carried out with seven, freshly prepared,
376 imprinted electrodes under the same conditions and an acceptable relative standard
377 deviation (RSD) of 4.1% was obtained. After each detection, the electrode was rinsed
378 with a water/methanol solution (4:6, v/v) to extract the analyte molecules. The RSD
379 for five repeated analyses using a single imprinted *PoAP*-PPY-MWNTs-BiCoPc-GC
380 electrode was calculated to be 5.3%, indicating that the sensor had good
381 reproducibility.

382 The stability of the imprinted *PoAP*-PPY-MWNTs-BiCoPc-GC electrode over
383 time was estimated over a month by weekly measurements of its current response
384 toward a 1.5×10^{-7} mol L⁻¹ MTMC test solution. A slight decrease in the relative
385 current change to about 88% of its initial value was found after the first two weeks of
386 storage in DDW at 4 °C, and it retained 83% of its initial value after one month of
387 storage. This good durability of the developed sensor is attributed to the rigid structure

388 of the imprinted PoAP membrane synthesized by electropolymerization and the
 389 excellent stability of the PPY-MWNTs-BiCoPc composite layer.

390 **3.7 Analysis of vegetable samples**

391 To demonstrate a feasible application of the fabricated imprinted
 392 PoAP-PPY-MWNTs-BiCoPc-GC electrode, cucumber and cabbage samples spiked
 393 with MTMC at three concentrations ($40.0 \mu\text{g kg}^{-1}$, $200.0 \mu\text{g kg}^{-1}$, $400.0 \mu\text{g kg}^{-1}$) were
 394 evaluated using the sensor. The concentration of MTMC was detected using three
 395 replicate measurements for each sample under the same conditions and the results are
 396 listed in Table 1. Good recoveries were obtained and ranged from 88.8 % to 93.3%
 397 with RSDs from 3.3 % to 5.1%, suggesting that the proposed sensor could accurately
 398 and reliably be used to analyze the MTMC residue in the vegetable sample.

Table 1. Recoveries of MTMC from spiked cucumber and cabbage samples, as determined by the developed electrochemical sensor

Vegetable samples	Spiked <i>conc.</i> ($\mu\text{g kg}^{-1}$)	Theoretical <i>conc.</i> ($\mu\text{g kg}^{-1}$)	Detected <i>conc.</i> ($\mu\text{g kg}^{-1}$)	Recovery %	RSD % (n = 3)
Cucumber	40.0	8.0	7.42	92.8	3.3
	200.0	40.0	36.40	91.0	4.2
	400.0	80.0	73.60	92.0	3.8
Cabbage	40.0	8.00	7.29	91.1	3.6
	200.0	40.0	35.52	88.8	4.0
	400.0	80.0	74.67	93.3	5.1

399 **4. Conclusions**

400 In this study, a novel PPY-MWNTs-BiCoPc composite layer and a molecularly
401 imprinted PoAP electrodeposited membrane were modified in a stepwise manner on a
402 GC electrode surface for the development of a MIP-based electrochemical sensor for
403 MTMC determination. We found that the PoAP-PPY-MWNTs-BiCoPc-GC electrode
404 performed well in the sensitive and selective determination of the target molecule.
405 This can be ascribed to a synergistic effect in the PPY-MWNTs-BiCoPc functional
406 layer and a number of selective binding sites in the imprinted PoAP membrane. The
407 sensor was found to have good reproducibility, long-term stability and could be used
408 to analyze for trace amounts of MTMC in spiked vegetable samples. This work
409 provides a convenient and inexpensive method for the preparation of sensing
410 elements and broadens the application of MIP-based sensors in the field of drug
411 residue determination.

412 **Acknowledgments**

413 This work was supported by the National Science Foundation for Distinguished
414 Young Scholars of China (project No. 31225021) and the Ministry of Science and
415 Technology of China (project No.2012AA101602) and Industry of quality public
416 welfare scientific research (project No. 201310146-3) and Special Fund for
417 Agroscientific Research in the Public Interest (project No. 201203069).

418 **References**

- 419 [1] D. Du, S. Chen, J. Cai and A. Zhang, *Talanta*, 2008, **74**, 766-772.
- 420 [2] D. G. Bracewell, A. Gill and M. Hoare, *Food Bioprod. Process.*, 2002, **80**, 71-77.
- 421 [3] B. J. Sanghavi, S. Sitaula, M. H. Griep, S. P. Kama, M. F. Ali and N. S. Swami,
422 *Anal. Chem.*, 2013, **85**, 8158-8165.
- 423 [4] P. A. Lieberzeit and F. L. Dickert, *Anal. Bioanal. Chem.*, 2009, **393**, 467-472.
- 424 [5] B. J. Sanghavi, O. S. Wolfbeis, T. Hirsch. T and N. S. Swami, *Microchim. Acta.*,
425 2015, **182**, 1-41.
- 426 [6] B. J. Sanghavi, S. M. Mobin, P. Mathur, G.K. Lahiri and A. K. Srivastava, *Biosen.*
427 *Bioelectron.*, 2013, **39**, 124-132.
- 428 [7] B. J. Sanghavi,, W. Varhue, J. L. Chavez, C. F. Chou and N. S. Swami, *Anal.*
429 *Chem.*, 2014, **86**, 4120-4125.
- 430 [8] E. Akyilmaz and E. Yorganci, *Biosens. Bioelectron.*, 2008, **23**, 1874-1877.
- 431 [9] B. Y. Wu, S. H. Hou, F. Yin, Z. X. Zhao, Y. Y. Wang, X. S. Wang and Q. Chen,
432 *Biosens. Bioelectron.*, 2007, **22**, 2854-2860.
- 433 [10] E. Pol, R. Karlsson, H. Roos, A. Jansson, B. Z. Xu, A. Larsson, T. Jarhede, G.
434 Franklin, A. Fuentes and S. Persson, *J. Mol. Recognit.*, 2007, **20**, 22-31.
- 435 [11] N. Liu, X. Chen and Z. F. Ma, *Biosens. Bioelectron.*, 2013, **48**, 33-38.
- 436 [12] A. Beltran, F. Borrull, P. A. G. Cormack and R. M. Marce, *Trac-trend. Anal.*
437 *Chem.*, 2010, **29**, 1363-1775.
- 438 [13] B. T. S. Bui and K. Haupt, *Anal. Bioanal. Chem.*, 2010, **398**, 2481-2492.
- 439 [14] K. Sreenivasan, *React. Funct. Polym.*, 2007, **67**, 859-864.

- 440 [15] A. McCluskey, C. I. Holdsworth and M. C. Bowyer, *Org. Biomol. Chem.*, 2007,
441 **5**, 3233-3244.
- 442 [16] D. Lakshmi, A. Bossi, M. J. Whitcombe, I. Chianella, S. A. Fowler, S.
443 Subrahmanyam, E. V. Piletska and S. A. Piletsky, *Anal. Chem.*, 2009, **81**,
444 3576-3584.
- 445 [17] G. P. Gonzalez, P. F. Hernando, and J. S. D. Alegria, *Anal. Bioanal. Chem.*, 2009,
446 **394**, 963-970.
- 447 [18] T. L. Panasyuk, V. M. Mirsky, S. A. Piletsky and O. S. Wolfbeis, *Anal. Chem.*,
448 1999, **71**, 4609-4613.
- 449 [19] A. Gomez-Caballero, M. A. Goicolea and R. J. Barrio, *Analyst*, 2005, **130**,
450 1012-1018.
- 451 [20] X. W. Kan, T. T. Liu, H. Zhou, C. Li and B. Fang, *Microchim. Acta.*, 2010, **171**,
452 423-429.
- 453 [21] R. S. Hutchins and L. G. Bachas, *Anal. Chem.*, 1995, **67**, 1654-1660.
- 454 [22] C. Malitesta, F. Palmisano, L. Torsi and P. G. Zambonin, *Anal. Chem.*, 1990, **62**,
455 2735-2740.
- 456 [23] S. Iijima, *Nature*, 1991, **354**, 56-58.
- 457 [24] R. T. Kachoosangi, M. M. Musameh, I. Abu-Yousef, J. M. Yousef, S. M. Kanan,
458 L. Xiao, S. G. Davies, A. Russell, and R. G. Compton, *Anal. Chem.*, 2009, **81**,
459 435-442.
- 460 [25] A. Benvidi, P. Kakoolaki, H. R. Zare and R. Vafazadeh, *Electrochim. Acta.*, 2011,
461 **56**, 2045-2050.

- 462 [26] H. Beitollahi, H. Karimi-Maleh and H. Khabazzadeh, *Anal. Chem.*, 2008, **80**,
463 9848-9851.
- 464 [27] J. F. Zang, C. M. Li, S. J. Bao, X. Q. Cui, Q. L. Bao and C. Q. Sun,
465 *Macromolecules*, 2008, **41**, 7053-7057.
- 466 [28] E. Pardieu, H. Cheap, C. Vedrine, M. Lazerges, Y. Lattach, F. Garnier, S. Ramita
467 and C. Pernelle, *Anal. Chim. Acta.*, 2009, **649**, 236-245.
- 468 [29] G. Z. Chen, M. S. P. Shaffer, D. Coleby, G. Dixon, W. Z. Zhou, D. J. Fray and A.
469 H. Windle, *Adv. Mater.*, 2000, **12**, 522-526.
- 470 [30] X. F. Li, S. Zhao, M. Yang, C. Q. Sun and L. P. Guo, *Thin Solid Films*, 2005,
471 **478**, 310-317.
- 472 [31] H. P. Li, J. H. Li, G. C. Li and J. F. Jen, *Talanta*, 2004, **63**, 547-553.
- 473 [32] J. Y. Ma, N. H. Lu, W. D. Qin, R. F. Xu, Y. B. Wang and X. N. Chen, *Ecotox.*
474 *Environ. Safe.*, 2006, **63**, 268-274.
- 475 [33] S. Y. Jin, Z. C. Xu, J. P. Chen, X. M. Liang, Y. N. Wu and X. H. Qian, *Anal.*
476 *Chim. Acta.*, 2004, **523**, 117-123.
- 477 [34] Q. H. Wu, G. Y. Zhao, C. Feng, C. Wang and Z. Wang, *J. Chromatogr. A*, 2011,
478 **1218**, 7936-7942.
- 479 [35] K. Qian, G. Z. Fang, J. X. He, M. F. Pan and S. Wang, *J. Sep. Sci.*, 2010, **33**,
480 2079-2085.
- 481 [36] J. W. Sun, B. Liu, Y. Zhang and S. Wang, *Anal. Bioanal. Chem.*, 2009, **394**,
482 2223-2230.
- 483 [37] J. W. Sun, T. T. Dong, Y. Zhang and S. O. Wang, *Anal. Chim. Acta.*, 2010, **666**,

484 76-82.

485 [38] Z. H. Zhang, Y. F. Hu, H. B. Zhang and S. Z. Yao, *J. Colloid Interf. Sci.*, 2010,

486 **344**, 158-164.

487 [39] L. Feng, Y. Liu, Y. Tan and J. Hu, *Biosens. Bioelectron.*, 2004, **19**, 1513-1519.

488 [40] Z. H. Zhang, Y. F. Hu, H. B. Zhang, L. J. Luo and S. Z. Yao, *J. Electroanal.*

489 *Chem.*, 2010, **644**, 7-12.

490 [41] D. M. Gao, Z. P. Zhang, M. H. Wu, C. G. Xie, G. J. Guan and D. P. Wang, *J. Am.*

491 *Chem. Soc.*, 2007, **129**, 7859-7866.

492 [42] C. G. Xie, Z. P. Zhang, D. P. Wang, G. J. Guan, D. M. Gao and J. H. Liu, *Anal.*

493 *Chem.*, 2006, **78**, 8339-8346.

494 [43] M. F. Pan, G. Z. Fang, B. Liu, K. Qian and S. Wang, *Anal. Chim. Acta.*, 2011,

495 690, 175-181.